JOURNAL OF Materials CHEMISTRY

Preparation, chemical stability, and electrical properties of $Ba(Ce_{1-x}Bi_x)O_3$ ($x = 0.0$–0.5)

Zhao Hui* and Pijolat Michèle

LPMG-CNRS 2021, Centre SPIN, Ecole Nationale Supérieure des Mines, 158 cours Fauriel, 42023 Saint Etienne cedex 2, France. E-mail: zhaohui98@yahoo.com

Received 27th May 2002, Accepted 24th September 2002
First published as an Advance Article on the web 15th October 2002

Solid solutions of the form $Ba(Ce_{1-x}Bi_x)O_3$ ($x = 0.0$–0.5) have been prepared by a modified Pechini method at 800 °C in air. XRD results indicate that all the samples have orthorhombic symmetry. $Ba(Ce_{1-x}Bi_x)O_3$ shows no reaction with $Ce_{0.9}Gd_{0.1}O_2$, even when sintered at 1100 °C, but totally decomposes when mixed with yttria-stabilized zirconia (8% Y_2O_3) and sintered at 900 °C in air. Compared to $BaCeO_3$, the chemical stability of bismuth-doped samples was improved in the presence of moisture. Bismuth substitution for cerium increases the total and electron conductivities. The total conductivity for $BaCe_{0.5}Bi_{0.5}O_3$ is 0.1 S cm^{-1} at 600 °C in air. Under oxidizing atmospheres, all the samples show p-type conducting properties, whereas in wet argon, the samples show both proton and electron conduction below 600 °C. The proton conduction decreased dramatically with increasing Bi content due to the compensation for oxygen vacancies by [$Bi_{Ce}^{\bullet}$] formed in the lattice. $Ba(Ce_{1-x}Bi_x)O_3$ exhibits a small cathodic overpotential, 70 mV at 800 °C in air at a current density of 100 mA cm^{-2}.

1 Introduction

It is well known that when the operating temperature of solid oxide fuel cells (SOFCs) is reduced to 600–800 °C, the reaction rate of the electrodes decreases dramatically, which may cause a huge overpotential at the electrode–electrolyte interface.[1–3] Many studies have focused on improving electrode performance. One way to overcome this problem is to form composite electrodes.[4–7] Generally, a highly electron-conducting phase, such as $La_{0.84}Sr_{0.16}MnO_3$ (LSM), is used as one composite and a highly ion-conducting phase, such as yttria-stabilized zirconia (YSZ) or doped CeO_2, is employed as the second. It is believed that the improved performance is due to the increased triple phase boundary (TPB) in the electrode–electrolyte interface.[8–11] Another way around the problem is to develop mixed ion- and electron-conducting materials. Many perovskite materials have been studied for this purpose, for example, $La_{1-x}A_xMO_3$ (A = Sr, Ca; M = Fe, Mn, Cr, Co)[12–14] and $Sr_{0.5}Sm_{0.5}CoO_3$[15–17] exhibit high cathode properties at intermediate temperatures. However, they are not suitable materials for SOFC applications, partly due to their ready reaction with YSZ to form an insulating phase, and partly due to cost considerations. The search for new cathode materials is still an ongoing challenge.

$BaCeO_3$ and related doped materials have been investigated as possible electrolytes for use at intermediate temperatures.[18–22] $BaCeO_3$ has been found to be unstable in the presence of moisture.[23] From the point of view of application, it is important to improve its chemical stability. Recently, it was reported that some doped $BaCeO_3$ materials can be used as cathodes in proton-conducting fuel cells.[24–26] Until now, very little attention has been paid to the possibility of using doped $BaCeO_3$ as cathodes in oxygen ion-conducting fuel cell systems. It is known that $BaCeO_3$ shows mixed proton and electron conduction in the presence of moisture, whereas in dry oxidizing atmospheres, it exhibits mixed oxygen ion- and electron-conducting properties.[18–22] Furthermore, research has revealed that fuel cell performance can be dramatically improved by using mixed oxygen ion- and proton-conducting materials as electrolytes.[27] It is therefore reasonable to assume that fuel cell performance can be further improved by using a mixed electron- and ion-conducting (both protons and oxygen ions) material. Doped $BaCeO_3$ appears to be a good candidate to fulfil this requirement.

In this study, we have investigated bismuth-doped $BaCeO_3$. The electrical properties of Gd and Bi co-doped $BaCeO_3$ have been studied previously,[28] and bismuth-doped $BaCeO_3$ has been prepared and its low temperature (<300 K) electrical behaviour investigated;[29] its high temperature properties, especially its possible use as a cathode material, have not been reported. Compared to a typical perovskite component, such as LSM (>100 S cm^{-1}), the reported total conductivity of doped $Ba(Ce_{1-x}M_x)O_3$ is relatively low [for example, it is 0.75 S cm^{-1} at 800 °C in air for $Ba(Pr_{0.8}Gd_{0.2})O_{2.9}$],[24] however, these materials exhibit low cathodic overpotentials.[24] Our purpose here is to investigate the effect of bismuth doping of $BaCeO_3$ on its chemical stability and electrical properties, and to assess the possible use of such materials as cathode materials in intermediate temperature SOFCs.

2 Experimental

2.1 Sample preparation

$Ba(Ce_{1-x}Bi_x)O_3$ solid solution was prepared by the Pechini method.[30] Typically, 0.01 mol $Ba(NO_3)_2$, 0.008 mol $Ce(NO_3)_3$, and 0.002 mol $Bi(NO_3)_3$ were mixed together, and then 0.04 mol citric acid and 20 ml deionized water were added to form a solution. The solution was dried at 120 °C and a transparent viscous liquid was obtained, the solution was then allowed to polymerize into a viscous brown liquid. Finally, the brown liquid was charred at 150 °C to form a dark brown resin and then the resin was heated at 800 °C for 4 h to give the final product. CGO ($Ce_{0.9}Gd_{0.1}O_2$) and YSZ (yttria-stabilized zirconia; 8% Y_2O_3) powders were provided by Rhodia and Superconductive Components, respectively.

Structural characterization was carried out by powder X-ray diffraction (XRD) on a Siemens D5000 diffractometer with Ni-filtered Cu-Kα radiation at room temperature. The scan rate was 0.1° (2θ) min^{-1}. KCl was used as an internal standard and the lattice parameters were refined by least-squares methods.

2.2 Chemical stability

In order to investigate the chemical stability of $Ba(Ce_{1-x}Bi_x)O_3$, powdered samples were mixed with CGO or YSZ (8%), in an equimolar ratio, and sintered at different temperatures in air. The chemical stability of $Ba(Ce_{1-x}Bi_x)O_3$ towards moisture was investigated by (i) immersing $Ba(Ce_{1-x}Bi_x)O_3$ powders in boiling deionized water or 1 M HCl aqueous solution for 24 h and (ii) exposing sintered pellets to wet argon at 800 °C for 24 h, the water partial pressure was fixed at 4.2 kPa by passing the argon through a water bath at 30 °C. The obtained products were examined by XRD.

2.3 Electrical measurements

For the electrical measurements, powders were pressed into compacts (8 mm in diameter and 2 mm in thickness) under 150 MPa. The pellets were sintered at 900 °C for 4 h in air, except for $BaCeO_3$, which was sintered at 1150 °C for 4 h. The sintered samples showed over 90% of the theoretical density determined by a water pyconmetric technique. Platinum paste (supplied by ESL Europe) was painted on two sides of the pellet as electrodes, and the disc with electrodes was sintered again at 850 °C for 2 h to remove the solvent. The electrical conductivity was measured on the sintered disc under a mixed dry nitrogen–air atmosphere and under wet argon. The oxygen partial pressure was determined with a Systech Instruments model 910 oxygen sensor. The water partial pressure was fixed at 4.2 kPa in the same way as described above. The conductivity measurements were performed using an ac complex impedance method at frequencies ranging from 5 Hz to 13 MHz on an HP4192A impedance analyser.

A polarization cell[31] was constructed to identify the transport species in dry atmospheres. The proton transport number was determined by the electromotive force (emf) method. A test cell was constructed according to ref. 25. Generally, one side of the pellet was exposed to wet argon and the other side to dry argon. From the measured emf and the Nernst equation, we can obtain the proton transport number, together with the total conductivity in wet argon, and the proton conductivity was calculated.

The oxygen reduction polarization at the $BaCe_{0.5}Bi_{0.5}O_3$ electrode was investigated in a three-electrode cell, using the current-interruption method to correct for the IR drop contribution. $Ce_{0.9}Gd_{0.1}O_2$ (CGO) was used as the electrolyte in this study. CGO powder was pressed and sintered at 1550 °C to form a dense pellet. $BaCe_{0.5}Bi_{0.5}O_3$ powder was first mixed with an organic binder (ethylene glycol) and then pasted on one side of the CGO pellet. The active electrode area was about 0.8 cm^2. Pt mesh (50 mesh) was pressed onto the surface of the $BaCe_{0.5}Bi_{0.5}O_3$ electrode to act as current collector. The pellet was heated up to 950 °C to form a contact interface between the $BaCe_{0.5}Bi_{0.5}O_3$ electrode and the CGO electrolyte. Pt paste was painted on the opposite side of the pellet and divided into two parts to form a counter and a reference electrode. The pellet was again was heated to 850 °C for 2 h to obtain porous Pt electrodes. The steady-state residual voltage between the $BaCe_{0.5}Bi_{0.5}O_3$ electrode and Pt reference electrode was monitored using an HP 54600B oscilloscope. The interruption current was supplied by a Solartron 1286 electrochemical interface. The polarization experiment was carried out at different temperatures in air.

3 Results and discussion

3.1 Phase formation and chemical stability

Fig. 1 shows the XRD patterns of resins heated at different temperatures in air. At 400 °C, the organic components are burnt off; the products formed are $BaCO_3$, α-Bi_2O_3, and CeO_2, no perovskite phase was observed. After heating at 600 °C for 4 h, the major phases were still $BaCO_3$, α-Bi_2O_3, and CeO_2, and a minor perovskite phase was detected and identified as $Ba(Ce_{1-x}Bi_x)O_3$. When the mixture was further heated to 800 °C for 4 h, pure $Ba(Ce_{1-x}Bi_x)O_3$ phase was formed, even for $BaCeO_3$, which was reported to be formed only at 1100 °C by solid-state reaction.[29] No impurities were detected and no superlattice structure was observed in the as-prepared bismuth-doped compounds. The XRD indexing results give orthorhombic symmetry for $Ba(Ce_{1-x}Bi_x)O_3$, with $x = 0.0$ to 0.5. Fig. 2 shows the change in cell parameters with bismuth content. Both the cell volume and cell parameters a, b, and c decrease with increasing bismuth doping content. Our results are in good agreement with the reported value for $Ba(Ce_{1-x}Bi_x)O_3$ prepared by solid-state reaction,[29] which indicates that homogeneous bismuth-doped $BaCeO_3$ solid solutions have been successfully prepared by the Pechini method.

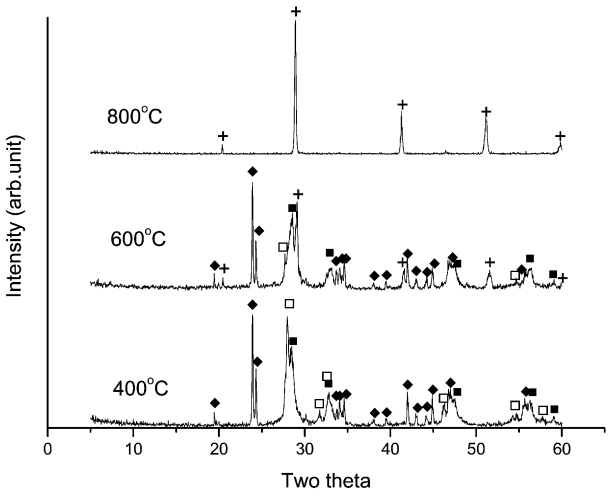

Fig. 1 XRD patterns of gels sintered at different temperatures. Key: (+) $BaCe_{0.5}Bi_{0.5}O_3$; (◆) $BaCO_3$ (JCPDF card no. 71-2394); (■) CeO_2 (JCPDF card no. 43-1002); (□) Bi_2O_3 (JCPDF card no. 27-0050).

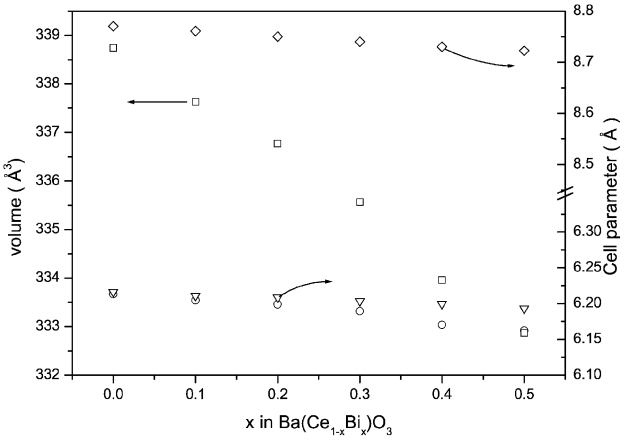

Fig. 2 Change in cell parameters with bismuth content in $Ba(Ce_{1-x}Bi_x)O_3$ solid solution ($x = 0.0$–0.5).

In order to investigate the chemical stability of $Ba(Ce_{1-x}Bi_x)O_3$ with the standard electrolytes yttria-stabilized zirconia (YSZ; 8% Y_2O_3) and $Ce_{0.9}Gd_{0.1}O_2$ (CGO), powdered samples were mixed with YSZ or CGO in equimolar ratios. The mixtures were heated at different temperatures in air and the XRD patterns of the sintered mixtures are shown in Fig. 3. $Ba(Ce_{1-x}Bi_x)O_3$ is stable when mixed with CGO, even when heated at 1100 °C for 12 h, since no reaction was detected. However $Ba(Ce_{1-x}Bi_x)O_3$ reacted with YSZ to form a fluorite structure

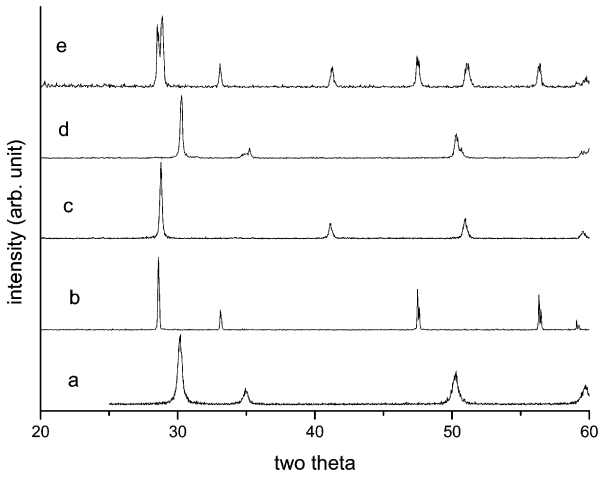

Fig. 3 XRD patterns of (a) as-received YSZ (8%), (b) CGO powder sintered at 1450 °C for 4 h, (c) $BaCe_{0.5}Bi_{0.5}O_3$ powder sintered at 800 °C for 4 h, (d) mixed $BaCe_{0.5}Bi_{0.5}O_3$ and YSZ powder sintered at 950 °C for 4 h, and (e) mixed $BaCe_{0.5}Bi_{0.5}O_3$ and CGO powder sintered at 1100 °C for 12 h.

solid solution at temperatures as low as 900 °C. Therefore, in the following experiments, we used CGO as the electrolyte.

Many papers have reported the chemical stability of rare earth-doped $BaCeO_3$ in wet atmospheres or in boiling water.[23,32–35] In this study, we investigated the effects of bismuth doping on the chemical stability of $BaCeO_3$. The XRD patterns of the resulting products are shown in Fig. 4. $BaCeO_3$ decomposed rapidly in boiling water and then reacted with water and dissolved CO_2 to give $BaCO_3$ and CeO_2, as has been reported by others.[23] With bismuth-doped samples, however, the chemical stability was dramatically improved. $BaCe_{0.5}Bi_{0.5}O_3$ shows no decomposition with water, even when heated at 100 °C in 1 M HCl solution for 24 h. $Ba(Ce_{1-x}Bi_x)O_3$ pellets were also exposed to wet argon at 800 °C for 24 h and the result was the same: no sign of decomposition or cracks in the pellets could be found.

It is known that the stability of the perovskite structure can be rationalized by the tolerance factor (t), which is defined according to eqn. 1,[36]

$$t = \frac{r_A + r_O}{\sqrt{2}(r_B + r_O)} \quad (1)$$

where r_A, r_B and r_O are the ionic radii of the A, B, and oxygen

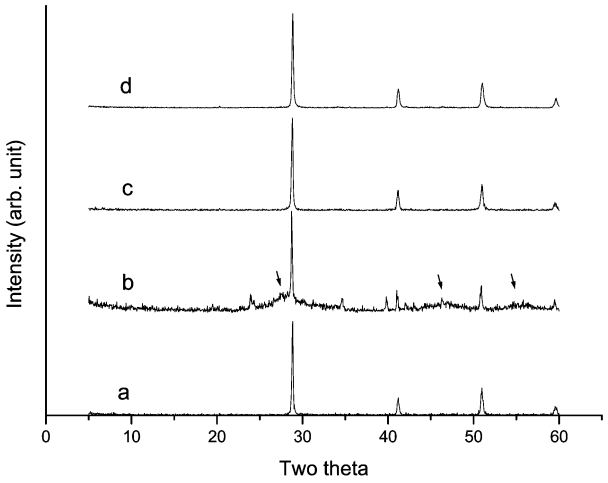

Fig. 4 XRD patterns of (a) $BaCeO_3$ before treatment, (b) $BaCeO_3$ treated in boiling water for 4 h (the arrows indicate peaks due to CeO_2), (c) $BaCe_{0.5}Bi_{0.5}O_3$ before treatment, and (d) $BaCe_{0.5}Bi_{0.5}O_3$ heated in1 M HCl solution at 100 °C for 24 h.

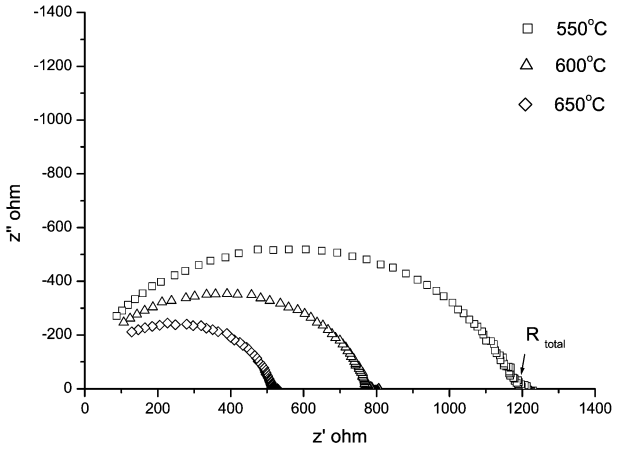

Fig. 5 A typical Cole–Cole plot for $BaCe_{0.9}Bi_{0.1}O_3$ measured in air.

ions, respectively. Some researchers have found that $BaCeO_3$ is not stable compared to its constituent oxides below 630 °C, due to the relatively low tolerance factor (about 0.89).[37] Generally, the closer to unity the value of t, the greater is the expected stability of the perovskite structure. Considering the random distribution of Bi ions in the lattice of bismuth-doped $BaCeO_3$,[29] and following the same procedure to calculate the tolerance factors of $AB'_{1/2}B''_{1/2}O_3$-type mixed perovskite proton conductors,[36] we find that t increase steadily from 0.89 for $BaCeO_3$ to 0.915 for $BaCe_{0.5}Bi_{0.5}O_3$ (here, the ion radii are: Ce^{4+} 0.97; Bi^{3+} 1.03; Bi^{5+} 0.74; Ba^{2+} 1.61; O^{2-} 1.4 Å), indicating the formation of a more compact lattice structure.

3.2 Electrical properties of $Ba(Ce_{1-x}Bi_x)O_3$

The electrical conductivity of $Ba(Ce_{1-x}Bi_x)O_3$ was measured by impedance spectrometry at different temperatures in air. Fig. 5 shows a typical Cole–Cole plot from our measurements. The conductivity was found to increase with increasing measurement temperature from 550 to 650 °C. Only one depressed arc exists from 1 MHz to 1 KHz, the contributions from grains and grain boundaries cannot be separated in this situation. The electrical conductivity of the bulk material was determined from the reciprocal of the resistivity at the lower frequency side intercept of the arc with the Z' axis, which gives the total conductivity (R_{total}) of the system studied. Fig. 6 shows the Arrhenius plot for $Ba(Ce_{1-x}Bi_x)O_3$ measured in air. A linear relationship was obtained below 600 °C for all the doped compounds. The total conductivity of $BaCe_{0.5}Bi_{0.5}O_3$ is 0.1 S cm^{-1}

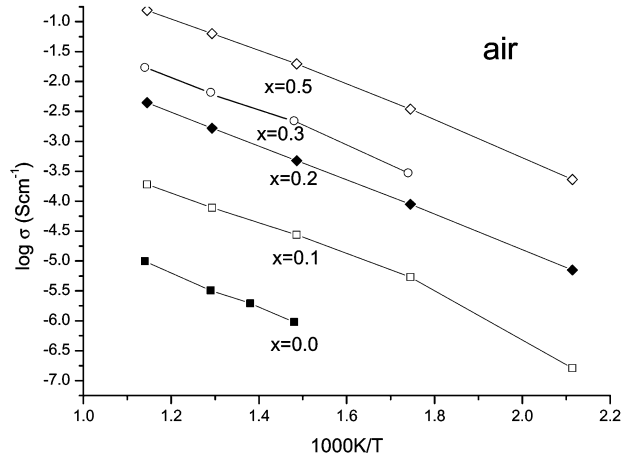

Fig. 6 Arrhenius plot of the conductivity of $Ba(Ce_{1-x}Bi_x)O_3$ solid solution (x = 0.0–0.5) measured in air.

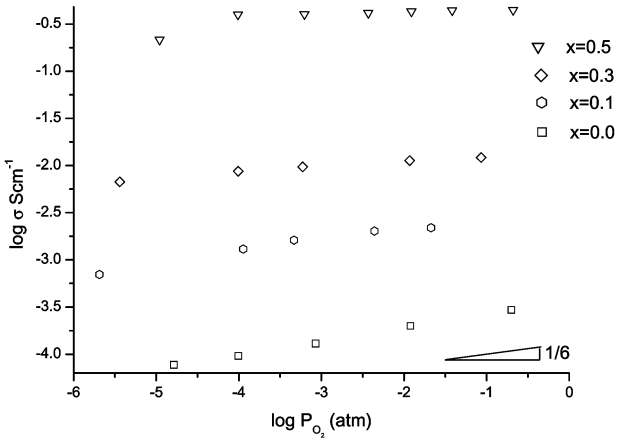

Fig. 7 Change in conductivity of $Ba(Ce_{1-x}Bi_x)O_3$ solid solution with oxygen partial pressure, measured at 650 °C.

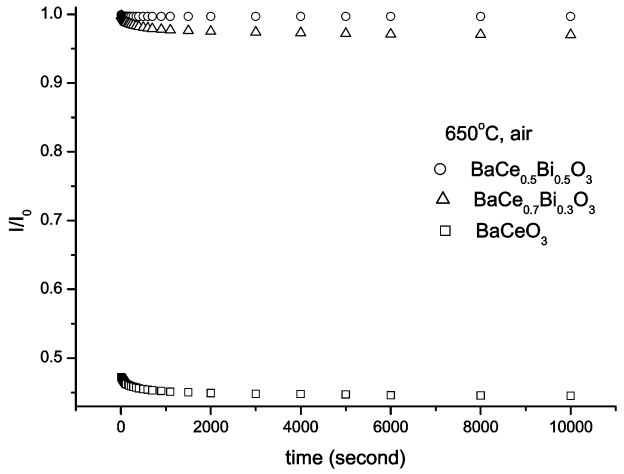

Fig. 8 Polarization curve of Au (block)/$Ba(Ce_{1-x}Bi_x)O_3$/Pt (porous) cell measured at 650 °C in air.

at 600 °C in air, comparable to the value reported by Mukundan *et al.* for the $BaCe_{1-x}Gd_xO_3$–$BaBiO_3$ system.[28] In our experiments, we observed that the total conductivity increased with increasing bismuth content and the activation energy remained almost unchanged (56.6 kJ mol^{-1} for $BaCeO_3$ and 53.2 kJ mol^{-1} for the $BaCe_{0.5}Bi_{0.5}O_3$). Our results follow the same trend as the conductivity of $BaCe_{0.5}Bi_{0.5}O_3$ measured at lower temperature,[29] a trend which was explained in terms of the competition between the bandwidth and charge disproportionation of bismuth ions in the lattice.

We also studied the dependance of R_{total} on the oxygen partial pressure. The results plotted in Fig. 7 show that R_{total} decreases with increasing oxygen partial pressure. For $BaCeO_3$, R_{total} is found to be proportional to $p_{O_2}^{1/6}$, indicating that $BaCeO_3$ is a p-type conductor in an oxidizing atmosphere and that the electric conductivity is a result of holes formed through the reaction shown in eqn. 2, as it has already been reported for the rare earth-doped $BaCeO_3$ system.

$$v_O^{\bullet\bullet} + 1/2O_2 \rightarrow O_O^x + 2h \quad (2)$$

With increasing bismuth content however, the conductivity changes little as the oxygen partial pressure is varied. For the $BaCe_{0.5}Bi_{0.5}O_3$, the conductivity remains almost unchanged in the whole range of oxygen pressure from 10^{-4} to 1 atm, indicating that hole transport is suppressed by the doping. It has previously been reported that both Bi^{3+} and Bi^{5+} ions exist in the $BaCe_{1-x}Bi_xO_3$ system,[29] moreover, it is known that Ce^{4+} ions can be reduced to form Ce^{3+} ions under low oxygen partial pressures. Thus, the oxygen vacancy will be compensated for according to eqn. 3 and 4 without formation of holes.

$$2CeO_2 + Bi_2O_3 \rightleftharpoons 2Ce_{Ce}' + 2Bi_{Ce}' + 2v_O^{\bullet\bullet} + 1/2O_2 + 6O_O^x \quad (3)$$

$$Bi_{Ce}' + v_O^{\bullet\bullet} + 1/2O_2 \rightleftharpoons Bi_{Ce}^{\bullet} + O_O^x \quad (4)$$

Therefore, the electric conductivity is mainly a result of hopping of electrons between Bi^{5+} and Bi^{3+}.

In order to confirm our explanation, we measured the dc polarization curve of a Au/$Ba(Ce_{1-x}Bi_x)O_3$/Pt cell. The results shown in Fig. 8 clearly indicate that no polarization phenomena exist for the bismuth-doped system, which further confirms that the major transport species in the bismuth-doped system is electrons.

In order to investigate possible proton transport in wet atmospheres for the bismuth-doped system, we constructed a test fuel cell. The proton conductivity is plotted in Fig. 9 as a function of bismuth content. The proton conductivity

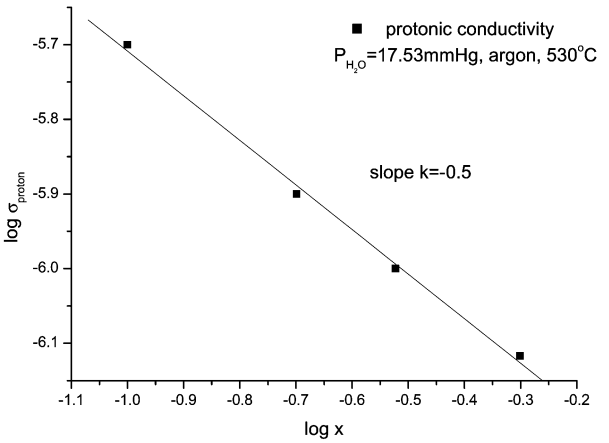

Fig. 9 Change in proton conductivity of $Ba(Ce_{1-x}Bi_x)O_3$ solid solution with bismuth content in wet argon.

decreases dramatically with increasing bismuth content. To explain such behaviour, we will consider the main defect reactions occurred in the doping system.

With eqn. 3, and the reaction of oxygen vacancies with water vapour (eqn. 5),

$$H_2O + v_O^{\bullet\bullet} \rightleftharpoons 2H^{\bullet} + O_O^x \quad (5)$$

the electrical neutrality condition requires

$$[H^{\bullet}] + [Bi_{Ce}^{\bullet}] + 2[v_O^{\bullet\bullet}] = [Ce_{Ce}'] + [Bi_{Ce}'] \quad (6)$$

According to Brouwer's approximation, when $[Bi_{Ce}^{\bullet}] \gg 2[v_O^{\bullet\bullet}] + [H^{\bullet}]$, eqn. 6 gives $[Bi_{Ce}^{\bullet}] = [Ce_{Ce}'] + [Bi_{Ce}']$. Then, applying the mass action law to eqn. 3 and 5 gives eqn. 7,

$$[H^{\bullet}] = K_1^{1/4}K_2^{1/2}p_{O_2}^{-1/8}p_{H_2O}^{1/2}[Bi_{Ce}^{\bullet}]^{-1/2} \quad (7)$$

where K_1 and K_2 are the equilibrium constants of eqn. 3 and 5, respectively, and are given by $K_1 = [Bi_{Ce}^{\bullet}]^2[v_O^{\bullet\bullet}]^2p_{O_2}^{1/2}$ and $K_2 = \frac{[H^{\bullet}]^2}{p_{H_2O}[v_O^{\bullet\bullet}]}$, respectively.

From eqn. 7, it can be seen that the proton concentration varies with the inverse square root of the bismuth content, which is in agreement with the experimental results (Fig. 9).

As $BaCe_{0.5}Bi_{0.5}O_3$ exhibits the highest electrical conductivity in the $Ba(Ce_{1-x}Bi_x)O_3$ series, we further investigated its possible use as a cathode material. The cathodic polarization was

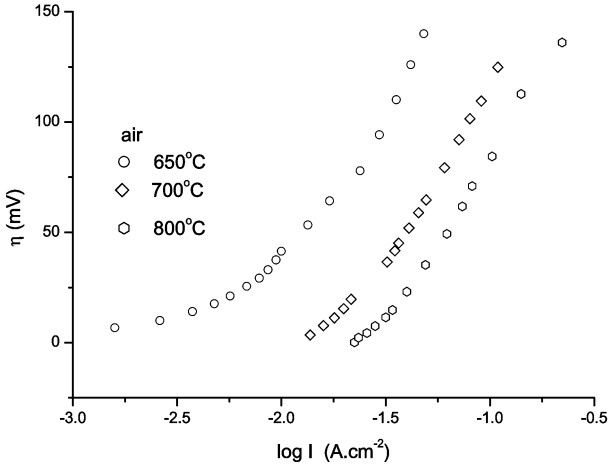

Fig. 10 Cathodic polarization curve for $BaCe_{0.5}Bi_{0.5}O_3$ measured at different temperatures in air.

measured from 700 to 800 °C in air, as shown in Fig. 10. At a current density of 100 mA cm^{-2}, the overpotential is found to be about 120 mV at 700 °C, and 70 mV at 800 °C. These values are in the same range as those reported for other excellent cathode materials, such as $Pb_2Ru_2O_{6.5}$ (161 mV at 700 °C at a current density of 100 mA cm^{-2})[38] and $La_{0.5}Sr_{0.5}MnO_{3-z}$ (55 mV at 800 °C at a current density of 100 mA cm^{-2}).[39] Further improvement of the cathodic properties could be obtained by forming a CGO–$BaCe_{0.5}Bi_{0.5}O_3$ composite electrode and by carefully tailoring the cathode morphology.

4 Conclusions

Bismuth-doped $BaCeO_3$ solid solutions have been prepared by the Pechini method at 800 °C. Bismuth doping both increased the electrical conductivity and enhanced the chemical stability of $BaCe_{1-x}Bi_xO_3$ in wet atmospheres. $BaCe_{1-x}Bi_xO_3$ did not react with $Ce_{0.8}Gd_{0.2}O_2$, even at 1100 °C, but totally decomposed when mixed with YSZ at 900 °C. Materials of the $BaCe_{1-x}Bi_xO_3$ series show p-type conducting properties in oxidizing atmospheres; the total conductivity of $BaCe_{0.5}Bi_{0.5}O_3$ is 0.1 S cm^{-1} in air at 600 °C. In a wet atmosphere, $BaCe_{1-x}Bi_xO_3$ exhibits mixed proton and electron conduction. The proton conductivity decreases with increasing bismuth content. The overpotential was found to be 70 mV at 800 °C in air at a current density of 100 mA cm^{-2}.

References

1 A. Endo, S. Wada, C. Wen, H. Komiyama and K. Yamada, *J. Electrochem. Soc.*, 1998, **145**, L35.
2 F. H. van Heuveln, H. J. M. Bouwmeester and F. P. F. van Berkel, *J. Electrochem. Soc.*, 1997, **144**, 126.
3 H. Uchida, H. Suzuki and M. Watanabe, *J. Electrochem. Soc.*, 1998, **145**, 615.
4 C. W. Tanner, K.-Z. Fung and A. V. Virkar, *J. Electrochem. Soc.*, 1997, **144**, 21.
5 T. Kenjo, S. Osawa and K. Fujikawa, *J. Electrochem. Soc.*, 1991, **138**, 349.
6 B. C. H. Steele, P. H. Middleton and R. A. Rudkin, *Solid State Ionics*, 1990, **40–41**, 388.
7 M. Mogensen, T. Lindegaard and U. Rud Hansen, *J. Electrochem. Soc.*, 1994, **141**, 2122.
8 E. P. Murray, T. Tsai and S. A. Barnett, *Solid State Ionics*, 1998, **110**, 235.
9 S. B. Adler, J. A. Lane and B. C. H. Steele, *J. Electrochem. Soc.*, 1996, **143**, 3554.
10 T. Inoue, N. Seki, K. Eguchi and H. Arai, *J. Electrochem. Soc.*, 1990, **137**, 2523.
11 K. Huang, M. Feng, J. B. Goodenough and M. Schmerling, *J. Electrochem. Soc.*, 1996, **143**, 3630.
12 N. Q. Minh, *J. Am. Ceram. Soc.*, 1993, **76**, 563.
13 L. Kindermann, D. Das, H. Nickel and K. Hilpert, *J. Electrochem. Soc.*, 1997, **144**, 717.
14 H. S. Issacs and L. J. Olmer, *J. Electrochem. Soc.*, 1982, **129**, 436.
15 M. Godickemerer, K. Sasaki, L. J. Gauckler and I. Riess, *Solid State Ionics*, 1996, **86–88**, 691.
16 H. Y. Tu, Y. Takeda, N. Imanishi and O. Yamamoto, *Solid State Ionics*, 1999, **117**, 277.
17 M. Koyama, C-J. Wen, T. Masuyama, J. Otomo, H. Fukunaga, K. Yamada, K. Eguchi and H. Takahashi, *J. Electrochem. Soc.*, 2001, **148**, A795.
18 N. Taniguchi, K. Hatoh, J. Niikura, T. Gamo and H. Iwahara, *Solid State Ionics*, 1992, **53–56**, 998.
19 H. Hu and M. Liu, *J. Electrochem. Soc.*, 1996, **143**, 859.
20 N. Bonanos, B. Ellis, K. S. Knight and M. N. Mahmood, *Solid State Ionics*, 1989, **35**, 179.
21 H. Iwahara, T. Esaka, H. Uchida and N. Maeda, *Solid State Ionics*, 1981, **3–4**, 359.
22 H. Iwahara, *Solid State Ionics*, 1988, **28–30**, 573.
23 C. W. Tanner and A. V. Virkar, *J. Electrochem. Soc.*, 1996, **143**, 1386.
24 R. Mukundan, P. K. Davies and W. L. Worrell, *J. Electrochem. Soc.*, 2001, **148**, A82.
25 R. Mukundan, P. K. Davies and W. L. Worrell, *Ceram. Trans.*, 1996, **65**, 13.
26 R. Mukundan, P. K. Davies and W. L. Worrell, *Mater. Res. Soc. Symp. Proc.*, 1997, **453**, 573.
27 B. Zhu, I. Albinsson and B. F. Mellander, *Solid State Ionics*, 2000, **135**, 503.
28 R. Mukundan, P. K. Davies and W. L. Worrell, *J. Mater. Res.*, 1999, **14**, 124.
29 R. J. Drost and W. T. Fu, *Mater. Res. Bull.*, 1995, **30**, 471.
30 H. Zhao, S. Feng and W. Xu, *Mater. Res. Bull.*, 2000, **35**, 2379.
31 T. Kawada, N. Sakai, H. Yokokawa and M. Dokiya, *Solid State Ionics*, 1992, **53–56**, 418.
32 S. V. Bhide and A. V. Virkar, *J. Electrochem. Soc.*, 1999, **146**, 2038.
33 L. N. Van Rij, J. Le, R. C. Van Landschoot and J. Schoonman, *J. Mater. Sci.*, 2001, **36**, 1069.
34 N. Taniguchi, C. Nishimura and J. Kato, *Solid State Ionics*, 2001, **145**, 349.
35 Z. L. Wu and M. L. Liu, *J. Electrochem. Soc.*, 1997, **144**, 2170.
36 S. V. Bhide and A. V. Virkar, *J. Electrochem. Soc.*, 1999, **146**, 4386.
37 S. Gopalan and A. V. Virkar, *J. Electrochem. Soc.*, 1993, **140**, 1060.
38 T. Takeda, R. Kanno, Y. Kawamoto, Y. Takeda and O. Yamamoto, *J. Electrochem. Soc.*, 2000, **147**, 1730.
39 Y. Takeda, R. Kanno, M. Noda, Y. Tomida and O. Yamamoto, *J. Electrochem. Soc.*, 1987, **134**, 2656.